

# Hyper-NA imaging of 45nm node random CH layouts using inverse lithography

E. Hendrickx<sup>\*a</sup>, A. Trichtkov<sup>b</sup>, K. Sakajiri<sup>b</sup>, Y. Granik<sup>b</sup>, M. Kempell<sup>c</sup>, G. Vandenberghe<sup>a</sup>

<sup>a</sup>IMEC, Kapeldreef 75, B-3001, Leuven, Belgium;

<sup>b</sup>Mentor Graphics Corp., 8005 SW Boeckman Rd., Wilsonville, OR 97070;

<sup>c</sup>Rochester Institute of Technology, 82 Lomb Memorial Drive, Rochester, NY 14623

## ABSTRACT

The imaging of Contact Hole (CH) layouts is one of the most challenging tasks in hyper-NA lithography. Contact Hole layouts can be printed using different illumination conditions, but an illumination condition that provides good imaging at dense pitches (such as Quasar or Quadrupole illumination), will usually suffer from poor image contrast and Depth of Focus (DOF) towards the more isolated pitches. Assist Features (AF) can be used to improve the imaging of more isolated contact holes, but for a random CH layout, an AF placement rule would have to be developed for every CH configuration in the design. This makes optimal AF placement an almost impossible task for random layouts when using rule-based AF placement. We have used an inverse lithography technique by Mentor Graphics, to treat a random contact hole layout (drawn at minimal pitch 115nm) for imaging at NA 1.35. The combination of the dense 115nm pitch and available NA of 1.35 makes the use of Quasar illumination necessary, and the treatment of the clip with inverse lithography automatically generated optimal (model-based) AF for all geometries in the design. Because the inverse lithography solution consists of smooth shapes rather than rectangles, mask manufacturability becomes a concern. The algorithm allows simplification of the smooth shapes into rectangles and greatly improves mask write time. Wafer prints of clips treated with inverse lithography at NA 1.35 confirm the benefit of the assist features.

**Keywords:** Contact hole imaging, inverse lithography, assist features

## 1. INTRODUCTION

The imaging of Contact Hole (CH) layouts is one of the most challenging tasks in hyper-NA lithography. Previous studies on CH imaging have shown that Quadrupole or Quasar illumination is suited best to control the Mask Error Factor (MEF) at dense pitches and thus provides the highest resolution.<sup>1,2</sup> The disadvantage of Quasar illumination is that it provides low Depth of Focus (DOF) and Exposure Latitude (EL) for the more isolated features. Fortunately, at Quasar illumination, the EL and DOF for dark-field CH layouts can be enhanced by the used of Assist Features (AF). The insertion of AF in a design is mostly done using rule-based scripting. Developing a rule for AF placement is relatively straightforward for patterns that consist of long 1-dimensional lines or spaces, but the complexity greatly increases when the pattern acquires periodicity in 2 directions, such as for regular CH arrays. For random CH arrays, writing a suitable rule for AF placement becomes an almost impossible task.

We have used inverse lithography to place model-based assist features for a random CH clip drawn at a minimal pitch of 115nm, and for Quasar illumination at NA 1.35. The inverse lithography, sometimes also referred to as pixel inversion, is a mask synthesis process that optimizes the mask shapes based on the optical image analysis for all image pixels in the work region. The mask synthesis is performed as a mathematical optimization process that minimizes a pixel-based objective function. The mask synthesis process typically produces main feature OPC shapes surrounded by SRAF shapes as well as, in some cases, “negative SRAF” inside the main feature OPC shapes. Details as to the definition of the objective function, as well as related techniques to solve the optimization problem through quasi-Newton method, are described in reference 3. The concept of the mask equalization through the high/low peak intensity leveling to achieve

larger common process windows as well as some of the early experimental results of inverse lithography are described in reference 4.

Raw optimization results of the pixel inversion generally contain polygons with lots of small features and arbitrarily angled edges. It's particularly problematic to have lots of small figures that cause not only mask-writing inaccuracy but also significantly increase the electron beam mask writer shot count. To address this issue, we have two somewhat different solutions. The first one is called geometrical mask simplification. The other one is what we refer to as the post pixel inversion MRC. While the geometrical mask simplification as a post process to the pixel inversion helps improve the manufacturability to some extent, it does not necessarily ensure that the result is clean in terms of MRC. The post pixel inversion MRC process takes the final pixel inversion result and tries to turn it into MRC-clean result while ensuring that resultant mask shapes would not cause undesirable imaging effects such as printing SRAF's. How exactly such simplification and MRC should be performed, however, is somewhat of open question due to complexities of the geometry with potentially conflicting conditions. In this paper, we explore some of those MRC/simplification options and provide some analysis on the resulting image quality, mask write time, and so on.

As experimental validation, the random CH clips with densest pitch 115nm and model-based AF were placed on a 6% AttPSM reticle, and printed at NA 1.35. We compare the difference between clips that had no AF, simplified model-based AF, and unsimplified model-based AF. The clips on the mask were inspected using reticle SEM to verify the AF presence and that their size was close to the target size. Limits for AF manufacturability and guidelines for mask simplification were derived from the reticle SEM mask inspection. We also demonstrate the ability of the AIMS<sup>TM</sup>-45 mask defect review tool to quickly provide intensity maps that correspond to the intensity seen by the scanner at wafer level. The reticle was then exposed on an ASML XT:1900i scanner (NA 1.35) using Quasar illumination. Both simulations and wafer data clearly show improved imaging of the random CH clip when treated with model-based AF and printed with Quasar illumination, compared to a clip that had no AF. The simplification of the AF only had a small impact on the imaging performance, but greatly improved mask write time.

## 2. MASKMAKING CONSTRAINTS

### 2.1 Inverse litho output and mask simplification

Figure 1 has an example of an inverse lithography conversion for a CH triplet in a random CH layout for Quasar illumination and 6% AttPSM. When unconstrained, the inverse lithography algorithm generates polygons with edges that consist of short straight segments at multiple different angles. In the inverted layout, the main CH features still have the largest area, but are no longer purely rectangular. At low magnification, the main CH features and AF appear as smooth shapes. In the inverse litho solution, the corner points of the vertices still fall on the design grid. Since the corner points are on the design grid, the maskshop theoretically is capable of manufacturing the mask. For the unconstrained inverse litho clip, a SEM image taken from a 6% AttPSM reticle is shown in Figure 1. Note that the total size of the clip was kept limited (6 by 7 micrometer at 1x).

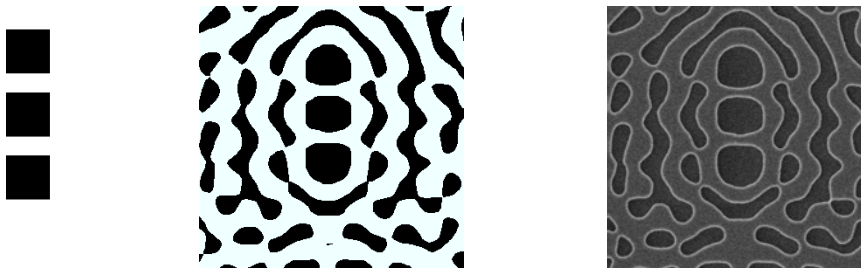
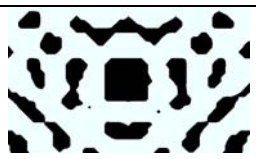





Fig 1: Left: Target layout (Here the wafer target CD was 80nm CH at 130nm pitch); Middle: inverse litho solution for Quasar illumination (30 degree opening angle, 0.93-0.69 sigma outer-inner) and 1.20NA; Right: Top-down reticle SEM image of the inverse litho clip as patterned on a 6% AttPSM.

The main difficulty with the unconstrained shapes is that mask write time would reach unreasonably high values if the shapes would cover the entire mask area. Gradual simplification of the unconstrained shapes to eliminate edges that are at angles not corresponding to 0 or 90 degrees, and by finally approximating each assist feature and contact hole as much as possible by a rectangular shape results in a drastic reduction of the mask write times. Table I has the mask write times that were simulated for a NuFlare EBM5000, assuming that an inverse litho design would fill the entire 4x mask area of 100 x 128 mm<sup>2</sup>. The write time simulated for the unconstrained inverse litho clip is 124 hrs. Replacing the CH polygons with rectangular shapes, as is normal for CH clips that have received OPC, and removing all edges that are not at 0, 45 or 90 degrees, already results in a reduction in runtime by a factor of 2.5. If, in addition, 45 degree edges are eliminated, mask write time reduces to 13.5hrs. A further reduction in mask write time by a factor of 2 is obtained by the use of MRC. Four types of MRC (Mask Rules Constraints) are implemented (min SRAF width, min SRAF area, min SRAF-to-SRAF space, min SRAF-to-Main Feature space). The image quality is monitored and adjusted if necessary during the MRC enforcement process.

Table 1: Different simplification levels of a pattern treated with inverse lithography, and resulting mask write time (simulated for NuFlare EBM5000), assuming that a layout would fill the entire mask area.

Clip type	Constraints	Mask Write time
	NONE	124 hrs
	Use rectangular CH Edges at 0, 45, 90 degrees only	51 hrs
	Use rectangular CH Edges at 0, 90 degrees only	13.5 hrs
	Use rectangular CH and AF Edges at 0, 90 degrees only Use MRC	6.5 hrs

## 2.2 Guidelines for MRC definition

When simplifying the mask, for example by eliminating all AF smaller than a given size, a set of rules has to be defined that reflect at minimum the capability of the maskshops to pattern the shapes. To set the optimal simplification rules, we have inspected a series of patterns on reticle using reticle CD-SEM (KLA 8250XR). Our main goal was to determine which minimal feature size and inter-feature distances should be respected.

For minimal feature size, several metrics can be used to define the minimal size of a 2D shape. First, when comparing the minimal AF dimension on reticle to the minimal desired AF dimension, no clear tendency was found in the deviations between the targeted and actual dimension. However, when an area-based analysis was used, a clear pattern emerged. The area based analysis was done by extracting the main CH and AF contours from a reticle SEM picture of an area with AF of multiple sizes and dimensions using Klarify Prodata. An extracted closed reticle contour can be integrated to obtain the area that we “get” on reticle for a certain CH or AF. From the reticle file or GDS, we can obtain the desired area, or “drawn” area for that feature. The difference between “drawn” area and “get” area is the area error

for that feature. If we plot the area error versus the desired or “drawn” area, we can see that the AF area error suddenly goes to large negative values if the “drawn” area drops below  $2000\text{nm}^2$  (at 1x). This corresponds to assist features smaller than a given “drawn” area gradually closing. The tendency is shown in Figure 2. Note that this exercise was conducted for 2 separate 6% AttPSM masks of identical layout, but fabricated at different maskshops. Both maskshops used 45nm node production tools for mask fabrication, and the results are very similar. Hence a first rule for assist feature cleanup is that the minimal assist feature area has to be larger than  $2000\text{nm}^2$  at 1x.

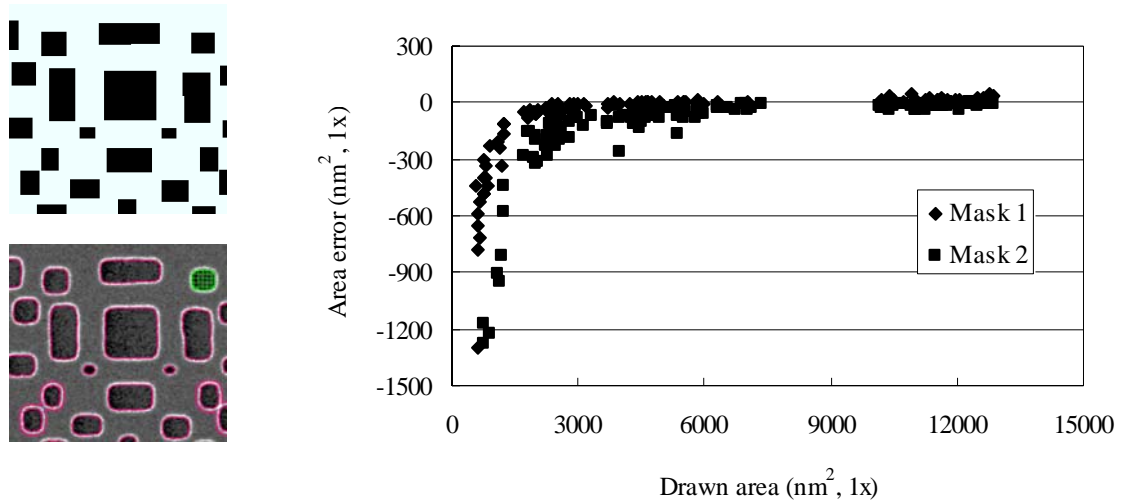


Figure 2: Left (top): GDS clip with AF of various size and aspect ratios; Left (bottom): Reticle SEM image, and extracted contours. The area of the AF in the top right corner is calculated by integration. This is the “get” area; Right: plot of the difference between “get” and “drawn” area versus “drawn” area. Note the sharp error increase if “drawn” area drops below  $2000\text{nm}^2$  (at 1x).

Similar rules have been determined for minimal distances between edges of CH and AF. By inspecting AF of various shapes and positions in the reticle SEM, and comparing the difference between “drawn” and “get” areas, we have seen on both masks that little interaction between AF or between AF and main features exists as long as the edges of the 2 features are apart by more than 30nm (at 1x). Hence our second rule for simplification is that edges have to be at least 30nm apart.

## 2.2 Mask inspection using AIMS<sup>TM</sup>-45

AIMS<sup>TM</sup>-45 is an optical reticle qualification tool. Using illumination conditions that are identical to those used in a full-field scanner (193nm wavelength and off-axis illumination), it captures images of the mask on a CCD camera at high magnification. If the AIMS<sup>TM</sup>-45 is used in scanner mode, it calculates the image as it would appear in resist at Hyper-NA and immersion conditions.<sup>5</sup> Whereas this tool is mostly used for reticle defect review, it is interesting to also compare AIMS images of patterns treated with different inverse lithography conditions. Since the image is formed using identical illumination conditions as in the scanner, and through the actual mask, possible reticle errors and reticle 3D effects are taken into account. In addition, the image is formed as an intensity profile, which gives information on maximal and minimal intensities inside and outside the CH. Minimal and maximal intensities are difficult to extract from wafer data. If the AIMS<sup>TM</sup>-45 image is acquired at multiple focus positions, information on contrast or NILS through focus can be extracted and compared to wafer process window data.

Figure 3 has AIMS<sup>TM</sup>-45 images (1.35NA, Quasar illumination) taken from a mask clip treated with traditional OPC (no AF, left), with simplified assist features placed using inverse lithography (middle), and with unsimplified AF (right). The densest pitch occurs in the CH triplet and is 115nm. Target CH CD was 70nm. All 3 images are at the same intensity scale. Note that traditional OPC gives very low overall contrast, with the lowest contrast present for the isolated AF. The simplified AF greatly improve the contrast of all contact holes. The image intensity map for the unsimplified AF (right) does not differ that strongly from the simplified AF. Note that even though the AF for the unsimplified case are large (see Figure 4 for the AF geometries), the background intensity at the position of the AF stays at a relatively low level. This means that the risk for assist feature printing stays low, even though the AF are fairly large. The images

demonstrate the ability of the inverse litho optimization routine to enhance the contrast of the main features using AF, whereas the background intensity or AF printing remains low. Considering the complexity of the 2D layout, this result would be very difficult to obtain using a rule-based approach.

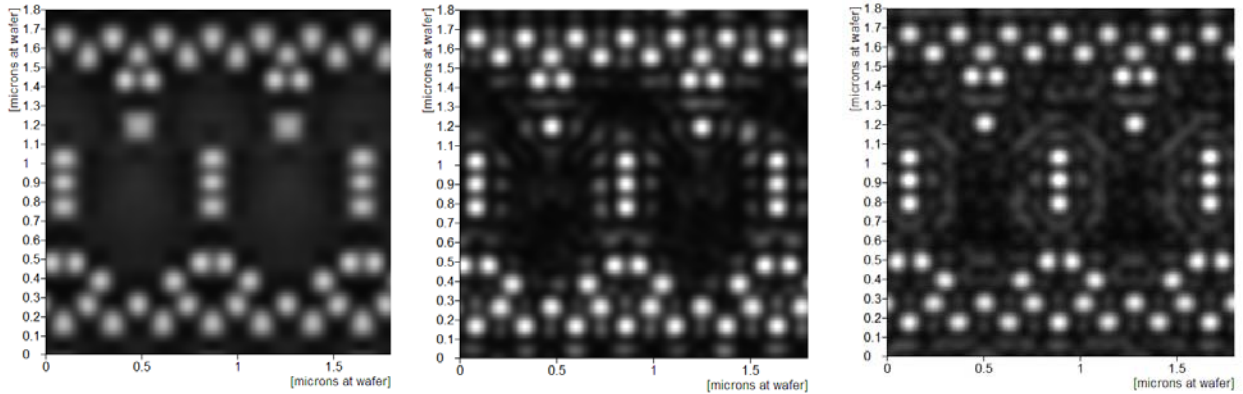


Figure 3: Scanner intensity as predicted by AIMSTM-45 (1.35NA, Quasar illumination) for a random CH clip and traditional OPC (left, no AF), simplified assist features placed using inverse lithography (middle), and unsimplified AF (right).

### 3. SIMULATION OF DIFFERENT TREATMENTS

A small clip of 5 by 7 micrometer (at 1x), and containing 500 random CH in random geometries, was treated using different inverse lithography conditions. The densest pitch was 115nm, and the target CD was 70nm. A small subsection of a target layout, and the resulting patterns after 3 treatments are shown in Figure 4. Again these treatments have been generated using regular OPC (no AF), applying simplified AF, and applying unsimplified AF.

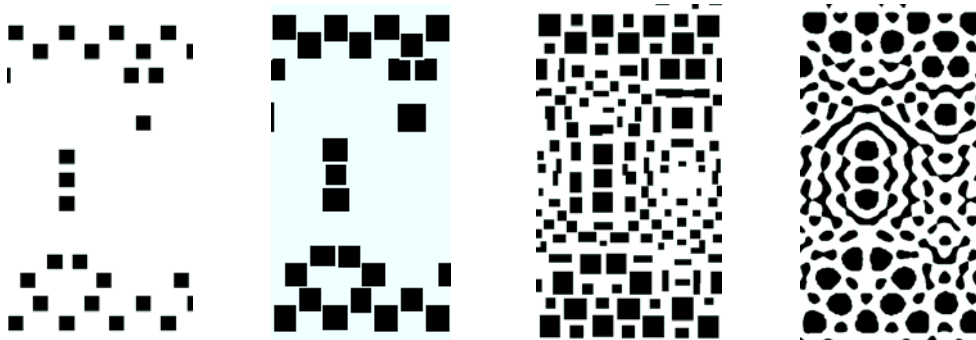


Figure 4: From left to right: (1) Target layout (densest pitch 115nm, 70nm target CD) (2) Traditional OPC treatment of the target clip. (1.35NA, Quasar illumination) (3) Clip after treatment with simplified assist features placed using inverse lithography (middle, MRC) (4) Clip after treatment with unsimplified AF (right).

For these 3 treatments, the CD change at multiple focus and dose conditions was simulated using OPC Verify. The simulation was done for Quasar illumination at NA 1.35. The dose was varied by +/- 10%, the focus variation was +/- 60nm. For a given CH, the area formed between the smallest CH contour (usually in defocus and low dose), and largest CH contour (usually in best focus and high dose) is called the Process Variation (PV) band. The area of the PV band is inversely proportional to the CD variation seen when going through focus and dose, and should be as small as possible. The areas of all PV bands of the entire clip can be placed in bins according to their sizes and this distribution is the so-called process variation band histogram. In Figure 5, we compare the process variation band histogram for the no AF case vs. that seen for the unsimplified AF treatment. Clearly, placement of the unsimplified AF results in a tremendous improvement in the process variation band histogram. Close inspection of the geometries in the different bins shows that the largest improvement occurs for the isolated contact holes. For the isolated CH without AF, the PV band areas are

almost completely in the highest 5 bins of the histogram. After placement of the unconstrained AF, the isolated CH shift to the smallest bins in the histogram for the unsimplified AF. The largest process variation bands for the unsimplified AF correspond to the CH in dense geometries and with diagonal neighbors. Diagonal geometries have poor process windows due to the use of Quasar illumination, and if the layout is too dense to generate AF, the inverse litho treatment can not improve printability. Here the only solution would be to omit these structures from the design. The shift in the PV band histogram matches what was seen in the AIMS<sup>TM</sup>-45 images.

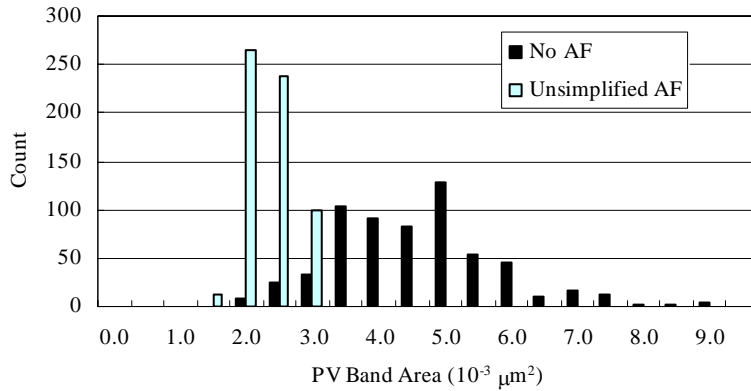


Figure 5: Process variation band histograms of the clip treated with traditional OPC and the clip treated with unsimplified AF.

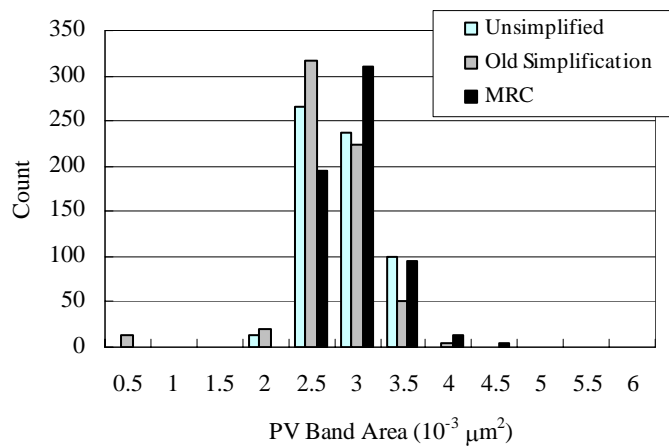


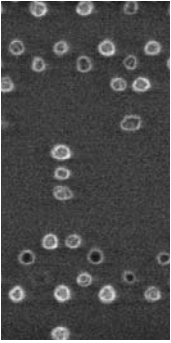
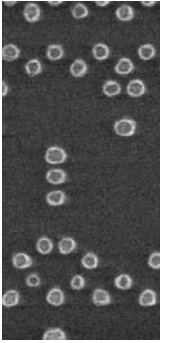
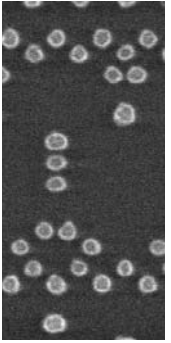
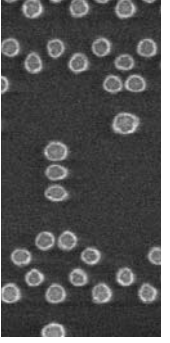
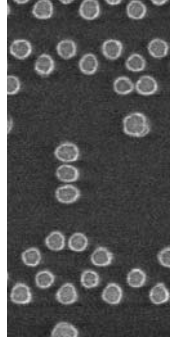
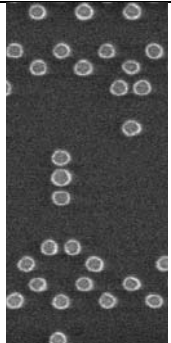
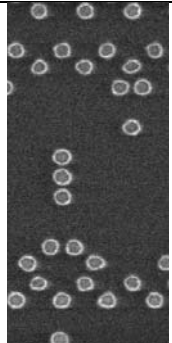
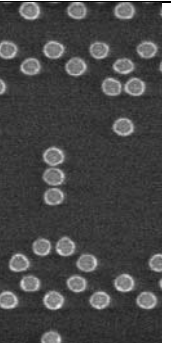
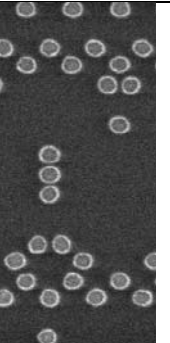
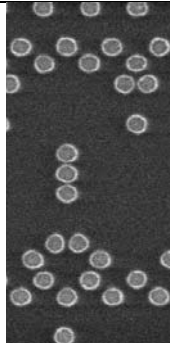
Figure 6: Process variation band histograms of the clip treated unsimplified AF, and 2 different types of AF simplification.

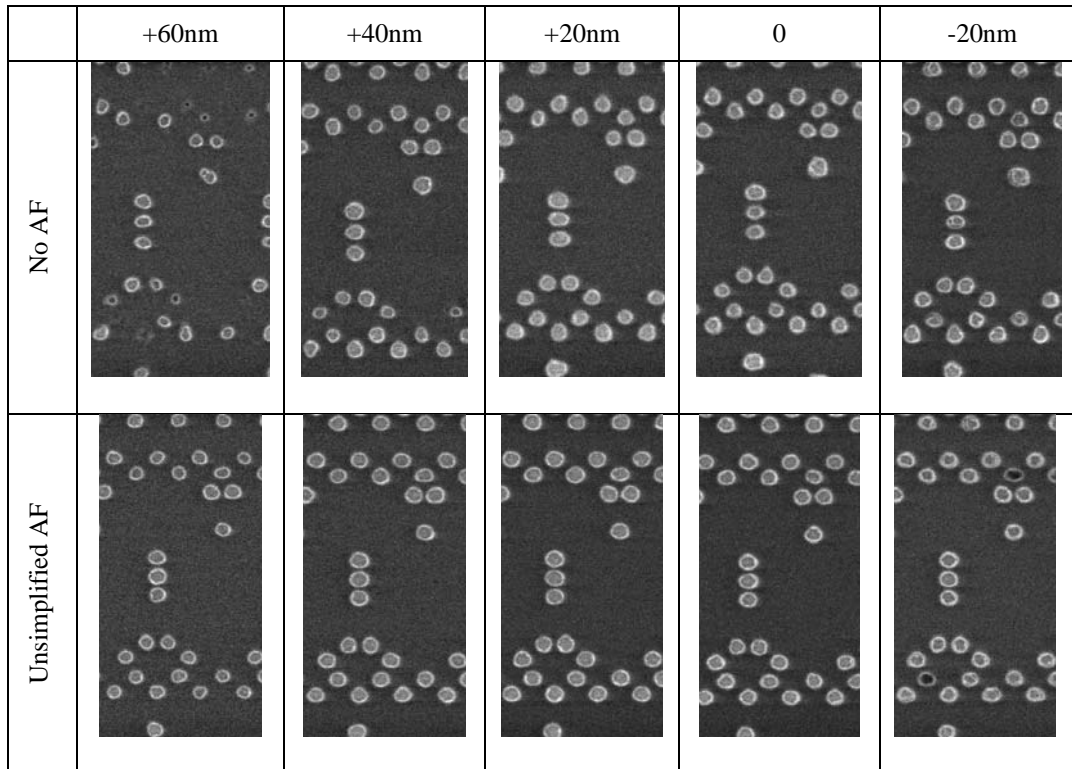
In Figure 6, we compare the PV band histogram for the clip that has the unsimplified AF (also shown in Figure 5) to those of 2 clips with AF of different simplification. The PV band histogram for the older simplification has additional peaks in the small PV band bins. Close inspection shows that these features correspond to printing AF. Here the simplification did not completely follow the shape of the unsimplified AF when the unsimplified AF was an elongated shape at diagonal orientation. For some areas, the incorrect simplification leads to printing AF. The MRC type simplification does much better in the approximation of diagonal AF, and as a consequence assist feature printing is no longer observed and the smallest histogram bins are empty. In the MRC, the geometries with multiple diagonal neighbors are still among those found having the largest PV bands, and the PV band area gradually decreases when the number of diagonal neighbors decreases and more space is available to insert assist features. The smallest PV bands are found for the dense and isolated CH.

#### 4. EXPERIMENTAL VALIDATION AT NA 1.35

The patterns in Figure 4 were exposed at 1.35NA, and using Quasar illumination. The top-down SEM images for the no AF case and the unsimplified AF case are shown in Figure 7. As could be anticipated from simulation and the AIMS™-45 images, there is a very strong performance improvement by using unsimplified AF.

In the No AF case, only the pattern at 12 mJ/cm<sup>2</sup> has reasonable fidelity. At higher or lower dose, the isolated CH and the CH in diagonal geometries no longer print properly. For the unsimplified AF, almost no pattern degradation is seen over the same exposure dose range. The same holds through for the evolution of the pattern through focus. Without AF, only the pattern at +20nm focus has reasonable fidelity, in positive or negative defocus the isolated and diagonal CH close and disappear. For the unsimplified AF cases, pattern fidelity is much better through focus. As was also seen in the simulations, even when using unconstrained AF placement, the diagonal geometries still have the lowest robustness for focus errors. The findings from wafer data confirm the tendencies seen in AIMS™-45 images and the simulations.

	10.8 mJ/cm <sup>2</sup>	11.4 mJ/cm <sup>2</sup>	12 mJ/cm <sup>2</sup>	12.6 mJ/cm <sup>2</sup>	13.2 mJ/cm <sup>2</sup>
No AF					
Unsimplified AF					



The process windows of the CH in selected geometries have been measured using KLA-T eCD2 CD-SEM using the CD2D algorithm. The data were processed in Klarity Prodata using a 70nm CD target and a  $\pm 7$ nm CD tolerance. Figure 8 has the graphs with maximal DOF and maximal EL for the CH indicated and labeled in the SEM picture. From the entire clip, we have selected CH geometries that represent the different bins in the PV band histogram. Here a quantitative comparison can be made of the different CH configurations and the impact of the different treatments. We can see that the treatment without AF has the lowest EL and DOF, and that the isolated CH without AF has the lowest printability. For EL, all geometries show a major improvement by placing either unsimplified or simplified AF. When comparing the EL for simplified and unsimplified AF, one tendency that can be seen is that the simplified AF have slightly more EL than the unsimplified AF, or that AF simplification leads to some loss in EL. A more detailed inspection of the AIMS<sup>TM</sup>-45 images shows a similar overall reduction in CH maximal EL upon AF simplification. When looking at the maximal DOF, the assist feature simplification causes some small changes in the DOF of the CH, but there is no systematic enhancement or reduction in DOF induced by the simplification. As was seen in the simulations and AIMS<sup>TM</sup>-45 images, the experimental data confirm that impact of the AF is the largest on the EL and DOF the isolated CH.

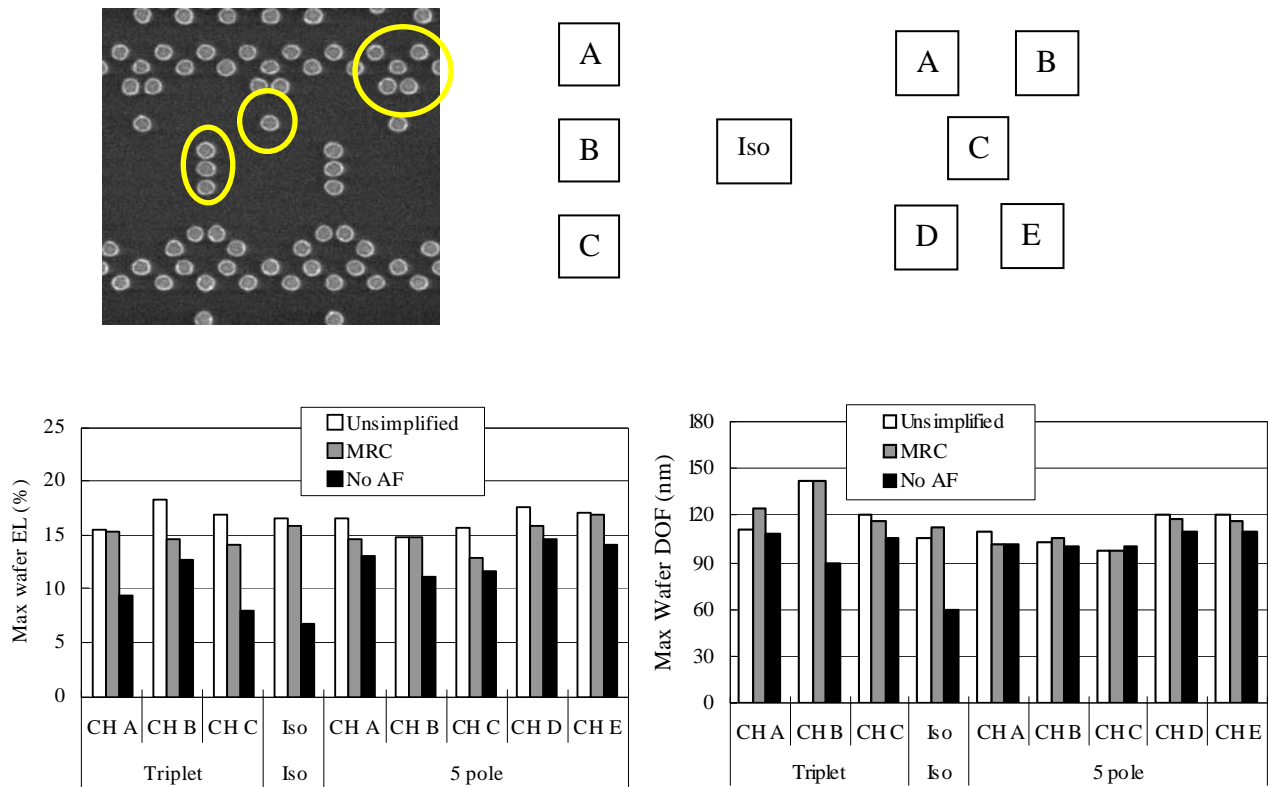


Figure 8: Top: Geometries for which the process window was determined, and legend to the labels in the graphs. Bottom left: Experimental maximal exposure latitudes for the CH in the different geometries. Bottom right: Maximal DOF for the CH in the different geometries.

## 5. CONCLUSION

We have demonstrated the ability of inverse lithography to successfully generate model-based assist features for a random CH clip and using Quasar illumination at NA 1.35. First conversions rapidly showed the need for pattern simplification to control mask write time. With moderate simplifications, simulated mask write times were found on the order of 12 hours. Reticle SEM measurements showed that good guidelines for MRC were the assist feature area (keep larger than  $2000\text{nm}^2$  at  $1\times$ ), and the minimal distance between the edges of the different features (keep larger than  $30\text{nm}$ ). Mask inspection was also done using AIMS<sup>TM</sup>-45 in scanner mode, which yielded an image as would be seen in resist at Hyper-NA conditions. The AIMS<sup>TM</sup>-45 images clearly demonstrated the overall contrast improvement with AF placement, while AF printability or the background intensity was still low.

Simulation of the different treatments was done using OPC Verify. Here the PV bands were calculated for different simplifications. Apart from again confirming the improvement in CH printability when using AF, the simulations also showed that simplification, when not properly done, can give rise to printing AF. The optimal MRC did not show any printing AF. A breakdown of the printing robustness by layout geometry revealed that CH in dense environments with multiple diagonal AF have the smallest benefit from inverse lithography. Here the dense geometry does not allow sufficient room for AF placement, and the diagonal neighbors reduce image contrast when using Quasar or Quadrupole

illumination. The simulations also show that isolated and dense CH have the largest process windows after inverse lithography.

A final check of the improvement of CH printing was done by wafer prints at 1.35 NA. The process windows of CH in selected geometries were measured using CD-SEM, and confirmed the tendencies seen in both simulations and AIMS<sup>TM</sup>-45. For the clip with simplified AF, the maximal EL were between 14-16%, and maximal DOF was from 95-140nm. Compared to the simplified AF, the unsimplified AF usually had slightly larger EL. Not placing AF did not give a workable solution, as could be expected for Quasar illumination.

**Acknowledgements** The authors would like to thank Eelco van Setten (ASML) and Remco Groenendijk (ASML) for help with the 1900i exposures; Won Kim (TI) for useful discussions; Peng Xie (RIT) for his help with the OPC Verify script; Joost Bekaert (IMEC), Jeroen Van De Kerckhove (IMEC), and Patrick Willems (IMEC) for their help with collecting the experimental data; Robert Birkner (Carl Zeiss) for his help with the AIMS<sup>TM</sup>-45.

## REFERENCES

- <sup>1</sup> V. Wiaux et al., "ArF solutions for low- $k_1$  back-end imaging" Proc. SPIE 5040, pp. 270-281 (2003)
- <sup>2</sup> J. Bekaert et al., "60nm half-pitch contact layer printing: exploring the limits at 1.35NA lithography" Proc. SPIE 6924 (2008)
- <sup>3</sup> C.Y Huang, Q. Liu, K. Sakajiri, S.D. Shang, and Y. Granik, "Model based insertion of assist features using pixel inversion method: implementation in 65nm node", Proc. SPIE 6283, 62832Y (2006)
- <sup>4</sup> Y. Granik, "Solving inverse problems of optical microlithography", Proc. SPIE 5754, 506-526 (2005)
- <sup>5</sup> P. De Bisschop et al., "Using the AIMS 45-193i for hyper-NA imaging applications", Proc. SPIE 6730, 67301G (2007)